(35) Hallock, S. A. Ph.D. Dissertation, The Ohio State University, 1974, p 90.
(36) Gray, H. B.; Billig, E.; Wojcicki, A.; Farona, M. *Can. J. Chem.* **1963**, *41*, 1281–1288.
(37) Blakney, B. G.; Allen, W. F. *Inorg. Chem.* **1971**, *10*, 2763–2770.
(38) Bamford, C. H.; Burley, J. W.; Coldbeck, M. *J. Chem. Soc., Dalton Trans.* **1972**, 1846–1852.
(39) Wrighton, M. *Chem. Rev.* **1974**, *74*, 401–430.
(40) While this process has not been studied in detail, UV spectral analysis indicates that the products are not those of $Mn_2(CO)_{10}$ or $[Mn(CO)_4Br]_2$, the latter being the reported product in benzene.[38]
(41) Waltz, W. L.; Akhtar, S. S.; Eager, R. L. *Can. J. Chem.* **1973**, *51*, 2525–2529.
(42) Owing to the strong near UV absorption of $Mn_2(CO)_{10}$ solutions, it was not feasible to observe at wavelengths below ca. 440 nm.
(43) Dorfman, L. M.; Adams, G. E. *Natl. Stand. Ref. Data Ser., Natl. Bur. Stand.* **1973**, *No. 46*.
(44) Fieldhouse, S. A.; Fullam, B. W.; Neilson, G. W.; Symons, M. C. R. *J. Chem. Soc., Dalton Trans.* **1974**, 567–569.
(45) Data for the $Mn(CO)_5Br$ case was that taken from the fourth to the eighth pulse because, as in the case of $Mn_2(CO)_{10}$, the decay rate decreased slightly from the first to the third pulse.
(46) Adams, G. E.; Michael, B. D.; Willson, R. L. *Adv. Chem. Ser.* **1968**, *81*, 289–308.
(47) In contrast to the transient behavior in the cases of $Mn_2(CO)_{10}$ and $Mn(CO)_5Br$, the decay rate of the transient for the $Mn(CO)_5I$ system was relatively insensitive to the number of irradiation pulses.
(48) Kidd and Brown[7] have proposed that $Mn(CO)_5\cdot$ can undergo rapid loss of CO; under our conditions, the decay of $Mn(CO)_5\cdot$ is second order. In addition, Hudson and co-workers[5] have proposed that $Mn(CO)_5\cdot$ can react with $Mn_2(CO)_{10}$ by electron transfer; however, our results indicate that if this reaction can occur it is much slower than reaction 6 under our conditions.
(49) Von Hartel, H.; Polanyi, M. *Z. Phys. Chem. (Frankfurt am Main)* **1930**, *11B*, 97–138.
(50) Anderson, O. P.; Symons, M. C. R. *J. Chem. Soc., Chem. Commun.* **1972**, 1020–1021.
(51) Reference 12b, p 124.
(52) Elian, M.; Hoffmann, R. *Inorg. Chem.* **1975**, *14*, 1058–1076.

Preparation of Chemically Derivatized Platinum and Gold Electrode Surfaces. Synthesis, Characterization, and Surface Attachment of Trichlorosilylferrocene, (1,1′-Ferrocenediyl)dichlorosilane, and 1,1′-Bis(triethoxysilyl)ferrocene

Mark S. Wrighton,* Michael C. Palazzotto, Andrew B. Bocarsly, Jeffrey M. Bolts, Alan B. Fischer, and Louis Nadjo

Contribution from the Department of Chemistry, Massachusetts Institute of Technology, Cambridge, Massachusetts 02139. *Received May 15, 1978*

Abstract: The synthesis and characterization of three ferrocene-centered, hydrolytically unstable, surface derivatizing reagents and their attachment to pretreated (anodized) Pt and Au electrode surfaces are described. Trichlorosilylferrocene (I) has been isolated from the reaction of $SiCl_4$ and lithioferrocene; (1,1′-ferrocenediyl)dichlorosilane (II) has been isolated from the reaction of $SiCl_4$ and 1,1′-dilithioferrocene; and 1,1′-bis(triethoxysilyl)ferrocene (III) has been isolated from reaction of $ClSi(OEt)_3$ with 1,1′-dilithioferrocene. The species I, II, and III have been fully characterized by ^1H NMR, mass, and UV–vis spectra and elemental analyses. All are moisture sensitive and are capable of derivatizing anodized Pt surfaces. Detailed studies for derivatization of anodized Au using II are described. In many respects the properties of derivatized Au electrodes parallel those for derivatized Pt. Such derivatized electrodes exhibit persistent cyclic voltammetric waves at a potential expected for an electroactive ferrocene derivative. Greater than monolayer coverages are found in each case, as determined by the integration of the cyclic waves. The cyclic voltammetric parameters are as expected for a reversible, one-electron, surface-attached electroactive system except that the peak widths are broader than theoretical. This is attributed to chemically distinct ferrocene centers resulting from the oligomerization of the derivatizing reagent during the derivatization procedure.

In a recent preliminary account we outlined the chemical derivatization of anodized Pt electrode surfaces using trichlorosilyferrocene (I), which resulted in the persistent attachment of polymeric, reversibly electroactive ferrocene.[1] Also, we have shown that (1,1′-ferrocenediyl)dichlorosilane (II) is capable of derivatizing n-type semiconducting Si photoelectrodes,[2] illustrating the first example of photoelectroactive surface-attached species. These studies have added to a growing literature of chemically derivatized electrode surfaces.[3-17]

Elaboration of the number and types of chemical derivatizing procedures is seemingly a necessary step in the illustration and understanding of fundamental and practical consequences of the resulting surfaces. In this article we wish to report the synthesis and characterization of I, II, and 1,1′-bis(triethoxysilyl)ferrocene (III) and their use as derivatizing reagents for anodized Pt electrode surfaces. We also report the first derivatized Au electrodes using II as the derivatizing reagent, and outline a procedure for the surface pretreatment of Au that leads to successful derivatization. The structures of the three derivatizing reagents are shown below. A qualitative comparison of the behavior of the resulting derivatized surfaces is made.

Results and Discussion

1. Preparation of Compounds. The compounds presented here are, by design, extremely moisture sensitive. Therefore, care must be taken in the exclusion of moisture in their preparation and subsequent handling. It should be noted that compounds I and II seem to react with glass over a period of time even when kept at low temperatures (−10 °C). Because of this problem, in order to obtain satisfactory analysis, the samples were purified immediately before being sent for analysis, sealed in plastic ampules under dry nitrogen, and analyzed as quickly as possible. This slow decomposition also requires that the compounds be purified before use in electrochemical studies.

All three complexes which we have prepared have been characterized by elemental analyses and the results are satisfactory. The mass spectral characterization provides a quick

0002-7863/78/1500-7264$01.00/0

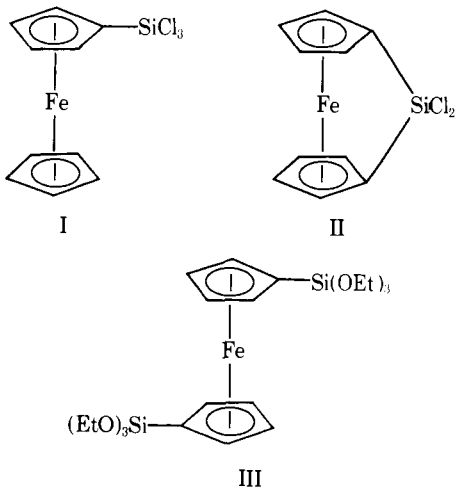

way to determine whether I, II, or III are present, since these complexes all give good parent peaks. For the complexes containing Cl's the parent peak region is complex and diagnostic owing to the characteristic distribution of ^{35}Cl and ^{37}Cl. ^1H NMR and electronic spectral data have also been used to characterize I, II, and III.

The low-energy absorption spectral features of the complexes prepared here are quite similar to those for ferrocene itself, which exhibits absorption maxima at λ 440 nm, $\epsilon \approx 90$, and 325 nm, $\epsilon \approx 50$.[18] Complex II exhibits a slightly red-shifted first absorption at ~470 nm and the shift is likely a consequence of distortion of the η^5-C_5H_5 ring systems from perfectly parallel; such has been found in the 1,1'-(ferrocenediyl)diphenylsilane analogue and it too has a red-shifted first absorption compared to ferrocene.[19] The first electronic absorption band has been attributed to a ligand field (d-d) transition and, consequently, should be sensitive to the geometry and nature of the immediate coordination sphere of the Fe.[18]

Similarity of the low-energy region of the electronic spectra of I-III and ferrocene itself is in accord with an expectation that the electrochemical oxidation would occur at a similar potential for each of the species. Indeed, many simply substituted ferrocenes have E^0 values in the vicinity of +0.4 V vs. SCE.[20] Complexes I and II are so moisture sensitive that solution electrochemical behavior is ambiguous. But complex III is qualitatively less reactive in solution, and its cyclic voltammetry in CH_3CN/0.1 M (n-Bu_4N)ClO_4 shows reversible waves establishing an E^0 of +0.47 ± 0.02 V vs. SCE.

2. Preparation and Characterization of Derivatized Electrodes. a. Surface Pretreatment. Pt electrode surfaces susceptible to derivatization with I-III have been prepared either by the procedure outlined in the literature[13a] or by a slight modification. For Pt disk electrodes the surfaces were hand polished to a mirror finish, anodized at +1.9 V vs. SCE for 5 min in 0.5 M H_2SO_4, and then cycled between the O_2 and H_2 evolution potentials in 0.5 M H_2SO_4 until the cyclic voltammograms were constant (~2 h). The electrode was then held at +1.1 V vs. SCE in that medium until the current declined to <1 $\mu A/cm^2$. Such a procedure presumably gives a hydrated Pt oxide surface capable of reacting with the Si-Cl or Si-OEt bonds of I-III.

Finding that the hand-polishing procedure was too labor intensive, we attempted the use of a procedure such that Pt foil electrodes could be prepared without polishing. Pt foil was cleansed in concentrated HNO_3 and then was anodized, cycled, and anodized as in the procedure for the Pt disk electrodes. Qualitatively, comparable results have been obtained with both types of Pt surfaces (vide infra).

Exposed Au surfaces were cleaned by dipping into concentrated HNO_3 for 5 min at 298 K. The electrode was then held at a potential of +1.9 V vs. SCE for 15 s in 0.5 M H_2SO_4 in H_2O. This was followed by cycling the potential (linear sweep, 100 mV/s) from 0.0 to +1.0 V vs. SCE until the cyclic voltammogram remained unchanged, 1-3 h. Finally, the potential was held at +1.9 V vs. SCE for 15 s. The electrode was then washed with distilled H_2O and then with acetone and allowed to dry in air.

b. Derivatizing Procedure. Pt surfaces to be derivatized were exposed to isooctane solutions of I-III under Ar as described in the Experimental Section. Au was derivatized with II in a similar fashion. The procedures actually used (reaction time, temperature, concentration of derivatizing reagent) were arrived at by trial and error. The one thing that is reproducible is that one can usually detect electroactive material after the derivatization, but the persistence, coverage, reversibility, etc., seem to depend on subtle factors not yet elucidated in the derivatizing procedure. Even carrying two electrodes through all procedures in parallel does not always yield electrodes having the same coverage of electroactive material.

c. Characterization of Derivatized Electrodes. Pt electrodes derivatized with I-III have been characterized by cyclic voltammetry in CH_3CN solutions of 0.1 M (n-Bu_4N)ClO_4 containing no deliberately added electroactive species. While all three derivatizing reagents do yield surface-attached electroactive material, there are some qualitative differences which are interesting. The data in Figures 1-4 and Table I are a collection of what we now regard as typical characteristics of Pt electrodes derivatized with I-III. Similar characterization of Au derivatized with II is provided by the data in Figures 5-9 and Table II.

First, that electroactive material is attached to the Pt or Au is unequivocally established by the observation of cyclic voltammetric waves in CH_3CN solutions containing no electroactive material; nonderivatized electrodes show no such waves in the potential window open in CH_3CN.

The position of the anodic and cathodic peaks, E_{ox} and E_{red}, respectively, for Pt electrodes derivatized with I-III are listed in Table I. That the surface-attached species are electroactive ferrocene derivatives is in accord with peak positions in the range 0.42-0.62 V vs. SCE. Surface attachment of reversibly electroactive species generally has not been found to effect large changes in the redox potential.[1-13] It is known that simply substituted ferrocene derivatives all have fairly similar E^0's;[20] ferrocene itself is measured to be +0.40 ± 0.02 V vs. SCE at a nonderivatized Pt electrode in CH_3CN/0.1 M (n-Bu_4N)-ClO_4, in our hands. The derivatizing reagents bearing only one Si atom, I and II, result in cyclic peaks at a more cathodic potential than from electrodes derivatized with III. The E^0 for III is more positive than for ferrocene itself, but unfortunately E^0's for I and II were not measurable.

For either derivatized Au or Pt electrodes, the area under the anodic and cathodic peaks is the same, revealing that the redox processes are chemically reversible. Several other characteristics point to kinetically reversible behavior as well. First, note that the peak to peak separations are below 59 mV in a number of cases at scan rates of 100 mV/s. At lower scan rates the peak to peak separation often approaches zero, as expected for a reversible surface-attached redox couple.[21] Further, the peak current is directly proportional to scan rate up to 500 mV/s and the peak to peak separation does not increase markedly at scan rates up to 500 mV/s. For solution species the peak current is predicted[22] and observed to be proportional to (scan rate)$^{1/2}$. Figures 1, 2, and 4 illustrate such information for Pt electrodes derivatized with II and III; similar data have already been published for Pt surfaces derivatized with I.[1] The data for Au derivatized with II are given in Figures 5 and 6.

One feature of the cyclic voltammetric waves is not in accord with the theory for a reversible, one-electron, redox couple

Table I. Electrochemical Data for Derivatized Pt Electrodes[a]

derivatizing reagent	expt	E_{ox}, V vs. SCE	E_{red}, V vs. SCE	coverage[b] × 10^{10}, mol/cm^2	$\Delta E_{1/2}$,[b,c] mV
I	1	+0.52	+0.50	3.9	400
	2	+0.48	+0.42	27.1	300
	3	+0.56	+0.53	60.0	340
	4	+0.54	+0.44	82.5	300
	5	+0.55	+0.43	49.7	240
	6	+0.53	+0.45	177	240
	7	+0.55	+0.46	286	270
II	1	+0.48	+0.44	9.3	250
	2	+0.47	+0.44	15.0	220
	3	+0.52	+0.49	28.6	260
	4	+0.53	+0.45	28.8	225
	5	+0.52	+0.44	29.3	380
	6	+0.53	+0.47	33.6	350
	7	+0.49	+0.44	33.7	220
	8	+0.48	+0.43	34.5	240
	9	+0.55	+0.53	52.2	240
	10	+0.53	+0.48	57.1	270
III	1	+0.61	+0.59	3.1	380
	2	+0.62	+0.58	4.8	540
	3	+0.58	+0.55	9.3	380
	4	+0.60	+0.57	14.6	320
	5	+0.59	+0.57	16.8	370
	6	+0.62	+0.58	19.9	390
	7	+0.61	+0.60	23.1	310

[a]Data presented here are from the 100 mV/s scan. [b]Calculated from the anodic wave. [c]Peak width at half height.

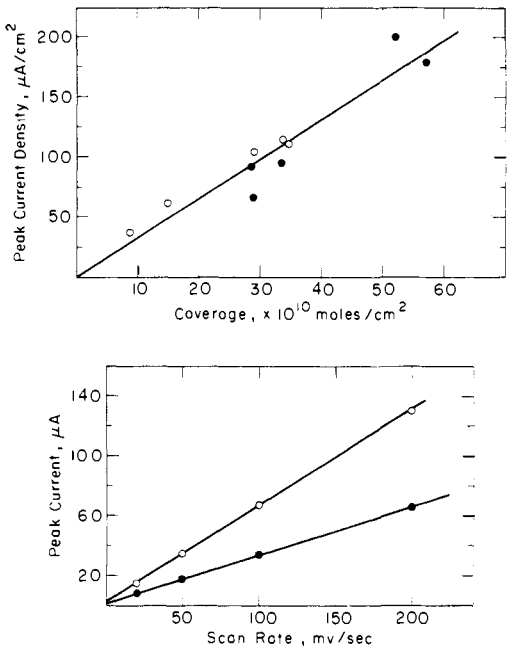

Figure 1. The upper graph shows a plot of peak current density vs. coverage at 100 mV/s for Pt electrodes derivatized with II. The open circles are for Pt foil electrodes and the closed circles are for Pt disk electrodes. Different amounts of coverage were achieved by varying the reaction time with II, but coverage at a given reaction time was not always reproducible. The lower graph shows a representative plot of anodic peak current vs. scan rate for two different Pt electrodes derivatized with II. Other conditions are as given in the Experimental Section.

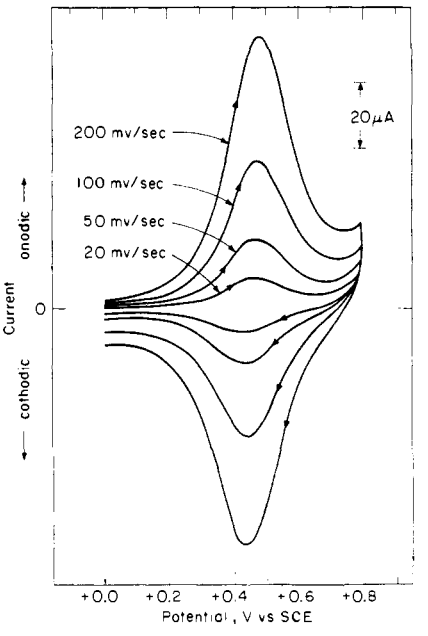

Figure 2. Results of a typical experiment measuring the scan rate dependence of the peak current for Pt electrodes derivatized with II.

attached to a surface. The width of the cyclic peaks at half-height should be ~90 mV according to theory,[21] but we find values in the range 170–540 mV. Further, over the range of coverages studied, the shape of the peaks is unchanged. This is evidenced by the linear plots of peak current against coverage: Figures 1 and 4 for Pt electrodes derivatized with II and III and Figure 6 for Au derivatized with II. Similar data obtain for Pt electrodes prepared using I and these have been published elsewhere.[1] Note that high coverages are obtainable; in several cases there appears to be coverage corresponding to tens of monolayers, given that the anodized Pt surface has ~10^{-10} mol/cm^2 of potential sites of attachment.[13a] However, even at coverages approaching monolayer, the shape of the cyclic peaks is still unchanged. We attribute the greater than monolayer coverages to oligomerization of I, II, or III in the derivatizing procedure according to chemistry as represented in eq 1. That is, there is attachment to the surface in certain positions, but there are oligomers formed via -O-Si-O-link-

Table II. Characteristics of Au Electrodes Derivatized with II

expt[a]	coverage × 10^9, mol/cm^2	E_{ox}, V	E_{red}, V	$\Delta E_{1/2}$,[b] mV	$\frac{1}{2}(E_{ox} + E_{red})$, V	E^0, V[c]
1	18.8	+0.475	+0.380	200	+0.430	+0.440
2	7.0	+0.475	+0.425	190	+0.450	+0.440
3	9.2	+0.480	+0.390	220	+0.435	+0.420
4	4.3	+0.465	+0.385	230	+0.425	
5	8.9	+0.475	+0.420	280	+0.450	+0.420
6	2.2	+0.420	+0.360	290	+0.390	
7	6.2	+0.460	+0.425	200	+0.440	+0.440
8	3.4	+0.420	+0.370	170	+0.395	
9	2.8	+0.450	+0.410	220	+0.430	+0.420
10	3.4	+0.450	+0.415	200	+0.430	+0.440
11	2.2	+0.520	+0.410	240	+0.465	
12	1.1	+0.450	+0.380	300	+0.415	
13	6.2	+0.490	+0.440	210	+0.465	+0.460
14	1.0	+0.500	+0.460	260	+0.480	
15	9.0	+0.480	+0.440	190	+0.460	
16	1.8	+0.430	+0.380	230	+0.405	
17	7.0	+0.485	+0.445	270	+0.465	
18	6.2	+0.480	+0.420	280	+0.450	
19	8.5	+0.490	+0.450	340	+0.470	
20	14.0	+0.490	+0.460	200	+0.475	+0.460

[a] All data in table recorded at 100 mV/s. Peak to peak separation usually smaller at slower scan rates. All potentials are referenced to an aqueous SCE. [b] Half-height width of anodic peak. [c] Determined using method outlined in text; see also Figure 8.

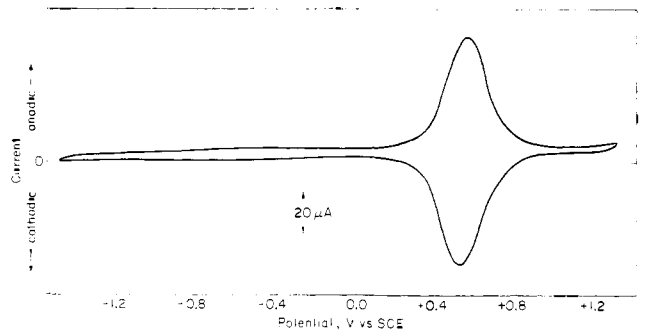

Figure 3. A Pt electrode derivatized with II cycled over a wide potential range without apparent loss of surface-attached material.

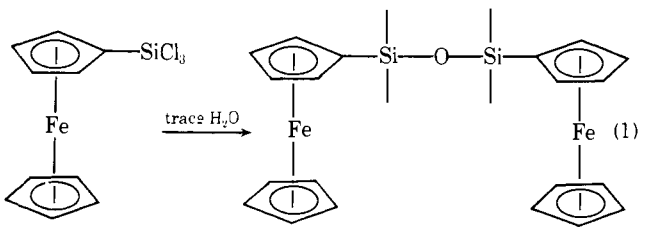

ages to involve ferrocene units which are not directly bonded to the metal surface. The important finding is that these oligomers are apparently reversibly electroactive. The broad cyclic peaks are explicable in terms of different ferrocene sites all having slightly different E^0's. Different sites on the surface and within the oligomer likely obtain. Support of this rationale is the observation that the cyclic voltammetric waves for polyvinylferrocene adsorbed on Pt are much sharper than those reported here;[15b] the ferrocene units in polyvinylferrocene are very likely nearly chemically equivalent, unlike the situation in the oligomers from I, II, and III.

Reagent II has some interesting possible modes of reaction not possible with I and III. The strained C-Si-C system makes the Si-C bond more reactive than usual, and chemistry as represented in eq 2 is not inconceivable. Tests for the presence of Si-bridged species are now underway using model compounds. Possible electronic interactions between the ferrocene

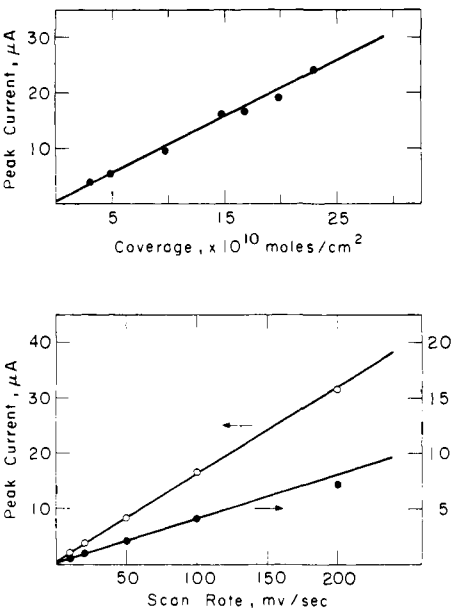

Figure 4. The upper graph shows a plot of peak current vs. coverage at 100 mV/s for Pt disk electrodes derivatized with III. Different amounts of coverage were achieved by varying the reaction time with III, but coverage at a given reaction time was not always reproducible. The lower graphs shows a representative plot of anodic peak current vs. scan rate for two different Pt electrodes derivatized with III. Other conditions are as given in the Experimental Section.

centers in such species may result in substantial changes in electrochemical behavior; dinuclear ferrocenes such as diferrocenylmethane give two cyclic voltammetric waves rather than one two-electron wave.[23] Data given in Table I suggest that no such chemistry obtains here, but occasionally derivatization with II has resulted in electrodes with *two anodic waves*. But such electrodes did not prove durable enough to completely characterize them and the results have been highly irreproducible.

Electrodes derivatized with I and II have been found to be extremely durable. Cyclic voltammetric scans between po-

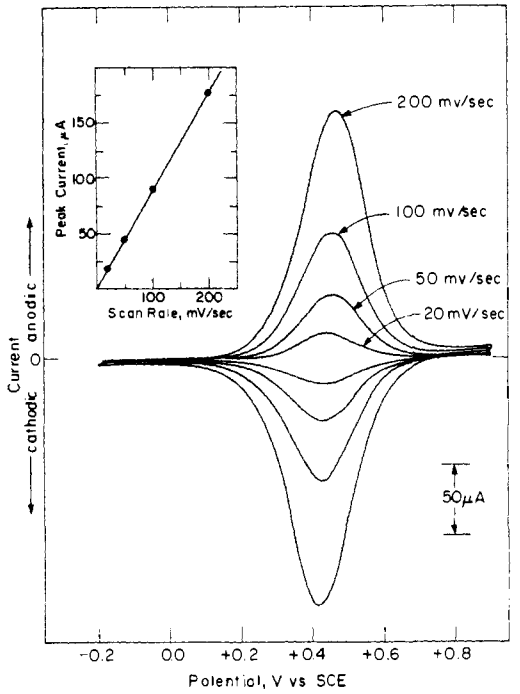

Figure 5. Cyclic voltammograms of derivatized Au as a function of scan rate in 0.1 M $(n\text{-}Bu_4N)ClO_4$ in CH_3CN under Ar at 298 K. Electrode coverage was 6.2×10^{-9} mol/cm^2. The inset shows a plot of peak anodic current against scan rate.

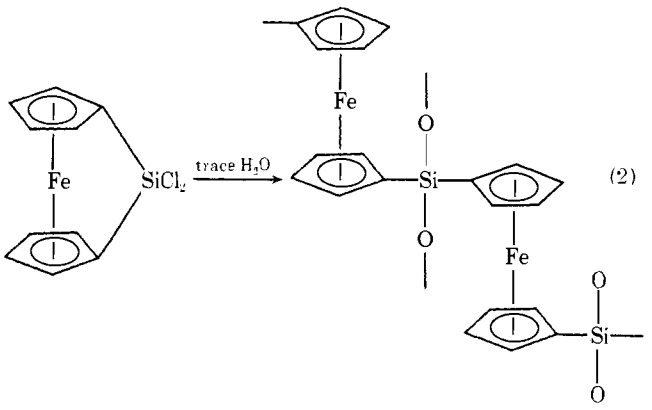

tentials where the electroactive material is reduced and oxidized can be carried out hundreds of times with only small loss of electroactive material. Shelf life of derivatized electrodes has exceeded 8 weeks without loss of electroactive material. Further, electrodes derivatized with I or II can be scanned over a very large potential window (Figure 3) without loss of the electroactive material. Persistence of electroactive material is not influenced by stirring the electrolyte solution. Obviously, however, mechanical abrasion of the surface does remove the electroactive material.

Pt surfaces derivatized with III are qualitatively less durable than those using I or II. It is more difficult to obtain high coverages which are persistently attached using III. Our data (Table I) show that the smallest coverages are obtained with III, even though the most forcing conditions are used in the derivatization procedure; cf. Experimental Section. Persistence of III is typically poor even over small potential excursions about E^0, as compared to surfaces derivatized with I and II. We attribute the difficulties of using III to its relatively low hydrolytic instability. III can be handled in air for short periods with no difficulty. Thus, the reaction of III with the pretreated surface is much slower. However, exactly why the resulting surfaces are not as durable is not clear. But from these qualitative finds, we conclude that our method of choice to derivatize anodized Pt is to use the reagents bearing Si–Cl bonds.

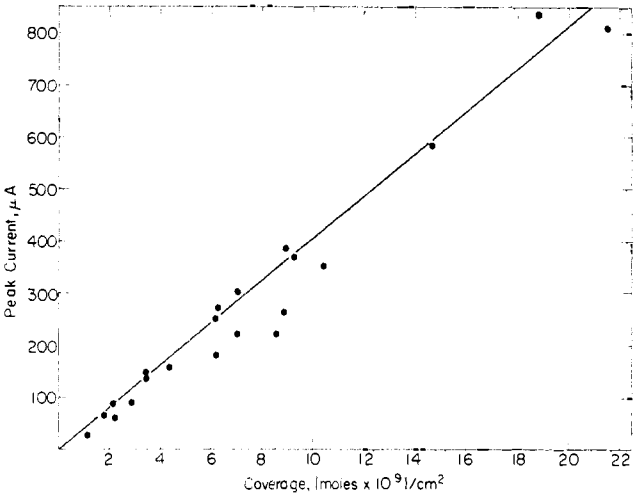

Figure 6. Plot of peak anodic current (100 mV/s) adjusted to 1 cm^2 electrode area, against electrode coverage for Au derivatized with II.

We find that derivatization of Pt foil or polished Pt disks results in surfaces which are quite comparable in all respects. One interesting find is illustrated in Figure 1, where data for foil and polished disks appear on the same graph; the data points fall on the same line. The nature of the pretreated surface, though, is consequential to the success of the derivatization procedure. Generally, the surface pretreatment procedure is necessary and gives electrodes having some attached electroactive material upon reaction with the derivatizing reagent. Derivatization using electrodes which have been cleansed in HNO_3 but not cycled or anodized does sometimes give derivatization, but the results are highly variable. Thus, it does appear that the oxide/hydroxide surface is needed. Such surfaces will not bind ferrocene itself by reaction in isooctane, revealing a necessary role for the Si–Cl and Si–OEt groups in derivatization.

d. Accurate Determination of E^0 for Derivatized Au Electrodes. For surface-attached, chemically and kinetically reversible, one-electron transfer systems, the E^0 is the potential at which the current reaches its peak value in the cyclic voltammogram.[21] For the present system, the E^0 values thus determined appear to be reasonable and fairly accurate. However, in some cases the peak to peak separation is not zero, or even close to zero, and it is not clear whether one should simply take as E^0 the average potential of the anodic and cathodic current peaks. Further, there may be electroactive material attached for which the electron transfer kinetics are sluggish, particularly when polymers are involved. Consequently, we have set out to measure the equilibrium surface concentration of oxidized and reduced material as a function of electrode potential; the procedure will be illustrated for Au and can be done as well for Pt. We define E^0 for the one-electron system to be simply that potential at which the concentration of oxidized and reduced forms is equal.

Measurement of equilibrium surface concentrations of oxidized and reduced species as a function of electrode potential has been carried out in the following manner. The derivatized Au electrode is stepped to a given potential and held there until equilibrium is established, i.e., until the current corresponding to oxidation or reduction of surface-attached species drops to zero. The electrode is then swept linearly in voltage either anodically (to measure the amount of reduced material) or cathodically (to measure the amount of oxidized material). The sweep is carried out slowly enough and far enough to ensure

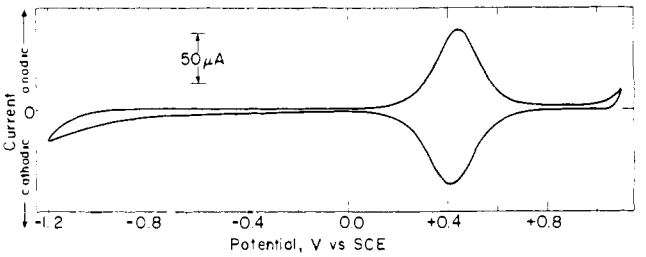

Figure 7. Cyclic voltammogram (100 mV/s) of a Au electrode derivatized with II (3.1×10^{-9} mol/cm^2) illustrating large potential excursions.

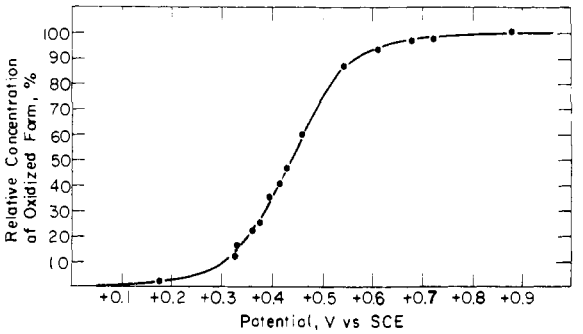

Figure 8. Example of plot of relative concentration of oxidized material against initial equilibrium potential as used to determine E^0. All data collected at 100 mV/s; cf. text.

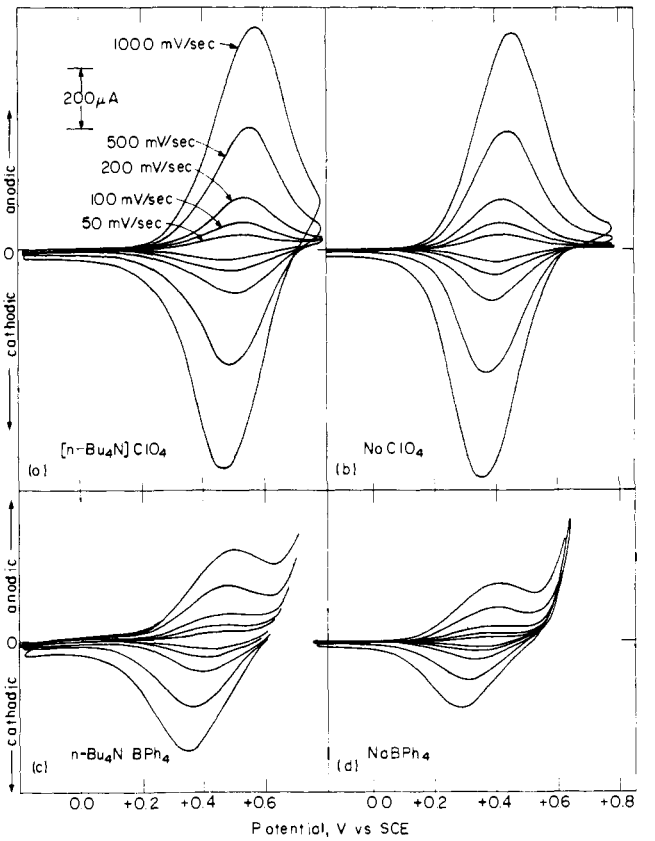

Figure 9. Cyclic voltammograms of a derivatized ($\sim 5 \times 10^{-9}$ mol/cm^2) Au electrode showing effects of four different electrolytes. All data collected using same electrode in a 0.1 M solutions of electrolyte in CH_3CN. Peak currents measured in 0.1 M (n-Bu_4N)ClO_4 in CH_3CN before and after (c) and (d) show a 15% loss in (d) which should be considered for an accurate comparison.

that all oxidized or reduced material is observed, i.e., the current drops to the background level. Integration of the current–time sweep then gives the needed information. A typical plot of the fraction of oxidized material as a function of the initial equilibrium potential for a derivatized Au electrode is given in Figure 8. The potential where there is 50% oxidized form is E^0, by our definition above. We have determined E^0 by this procedure for a number of derivatized electrodes, and these data along with the average of the peak potentials are included in Table II. For these systems it appears that the E^0 values are fairly constant and agree very well, as expected, with the E^0 from the cyclic peak positions.

e. Supporting Electrolyte Dependence for Derivatized Au Electrodes. Large coverages of electroactive material suggest the possibility that there is a large effect on the electrochemistry with variation in the supporting electrolytes. This follows from the realization that the oxidation of each ferrocene unit requires the presence of a nearby counteranion. Effects could be especially large for the highest coverages where considerable ion penetration into a derivatizing film is seemingly required. Indeed, for very high coverage electrodes, we observe that high scan rates in cyclic voltammetry do tend to show larger peak to peak separation and broader peaks; this might be a consequence of slow ion diffusion in and out of the derivatizing film. In this section we outline some preliminary results for derivatized Au which quite clearly show supporting electrolyte effects. But a detailed analysis must await a more complete study.

Figure 9 shows the cyclic voltammograms for a derivatized electrode at modest coverage (3×10^{-9} mol/cm^2) using four different supporting electrolytes. The study is by no means complete, but we draw attention to the fact that a very substantial effect can be seen in comparing (n-Bu_4N)ClO_4 with (n-Bu_4B)BPh_4 and $NaClO_4$ with $NaBPh_4$. There is little effect associated with the cation (Na^+ vs. (n-Bu_4N)$^+$) but there is a large effect in changing ClO_4^- to BPh_4^-. We determined that the cyclic voltammetry of ferrocene at naked Au is essentially independent of whether the electrolyte is (n-Bu_4N)ClO_4 or $Na(BPh_4)$. Further, a solution containing 0.05 M ClO_4^- and 0.05 M BPh_4^- gives nearly the same behavior as 0.1 M ClO_4^-. Finally, the attenuation effect of BPh_4^- is completely reversible.

At this point, we offer the tentative rationale that the anion effect is due to a size effect. However, we have no reason at this point to rule out certain other possibilities including solubility of the anion in the film. The lack of complete attenuation of the cyclic waves may be attributed to irregularities in coverage (thickness, permeability, etc.) which allow BPh_4^- easy access to some, but not all, ferrocene centers which are simultaneously close enough to the Au to be oxidized.

Some additional supporting electrolytes have been used including (Et_4N)ClO_4, (Me_4N)ClO_4, and (n-Bu_4N)PF_6. In comparing these to (n-Bu_4N)ClO_4, we find only modest shifts in cyclic peak positions, area, and shape for the same derivatized electrode, but there are no effects as large as found with BPh_4^-.

f. Nature of Pretreated Au Surfaces. Attachment of II to Au surfaces which are not pretreated according to the procedure outlined above has not worked reliably in our hands. Thus, we attach some significance to the formation of some sort of Au oxide/hydroxide surface in the pretreatment procedure. The anodized Au surface is believed[24] to be some form of Au_2O_3 and some degree of hydration of the anodized surface apparently provides the sites of attachment necessary to bind the hydrolytically unstable species II and also allows the growth and/or precipitation of the polymeric material. Electron spectroscopic analyses of clean, pretreated, and derivatized Au electrodes are underway to characterize the surface species.

Summary

Pretreated (anodized) Pt foil, polished Pt disks, or Au can be modified with ferrocene derivatives bearing Si–Cl or Si–OEt groups. Derivatization yields greater than monolayer coverages, and the persistence of the Pt surfaces is best for the derivatizing reagents having Si–Cl bonds. Attachment of oligomeric quantities of ferrocene derivatives is likely via M–O–Si–ferrocenyl (M = Au, Pt) linkages; the oligomers are the result of Si–O–Si bonds, and not all electroactive units need be attached directly to the surface. Chemically distinct ferrocene units contribute to broad cyclic voltammetric peaks, but reversible electrochemical behavior is observed even for coverages in the tens of monolayer range.

Experimental Section

1. Preparation of Compounds. All manipulations were done under inert, dry atmosphere using standard Schlenk line techniques. Solid transfers were made in a Vacuum Atmospheres drybox. All solvents were freshly distilled from sodium/potassium benzophenone ketyl under argon before use. *N,N,N′,N′*-Tetramethylethylenediamine (TMEDA) was distilled from BaO under argon before use. Silicon tetrachloride was freshly distilled from molecular sieves before use. Chlorotriethoxysilane (Petrarch Research Systems, Inc.) was used as received. Ferrocene was recrystallized from hexane and chloromercuriferrocene (ROC/RIC) was used as received. Elemental analyses were performed by Galbraith Laboratories, Inc.

a. Trichlorosilylferrocene (I). Chloromercuriferrocene (0.051 mol) was converted into the monolithioferrocene.[25] This product was not isolated. The monolithioferrocene was dissolved in DME and added slowly, over a period of several hours, to an excess of $SiCl_4$ (25 mL, 0.22 mol). The reaction mixture was allowed to stir for an additional 3 h before the solvent and unreacted $SiCl_4$ were removed under vacuum. The resulting yellow solid was dissolved in pentane and filtered to remove LiCl and the solvent was removed under vacuum. The product was purified by vacuum sublimation (0.1 mm); ferrocene sublimed at room temperature, and the desired product sublimed when the temperature was increased to 50 °C. This procedure gave 4 g, 25% yield, of I, a yellow, crystalline solid: mp 75–77 °C; UV max (isooctane) 440 nm (ϵ 140), 324 (110); NMR (C_6D_6) 4.02 (s) and 4.13 (m) ppm downfield from Me_4Si; mass spectrum *m/z* (rel intensity) 316 (8.85), 317 (2.65), 318 (100), 319 (19.91), 320 (96.46), 321 (18.14), 322 (34.07), 323 (7.08), 324 (5.31).

Anal. Calcd for $C_{10}H_9FeSiCl_3$: C, 37.58; H, 2.82; Cl, 33.35; Si, 8.77; Fe, 17.49. Found: C, 37.82; H, 2.90; Cl, 33.58; Si, 8.51; Fe, 17.65.

b. 1,1′-Dilithioferrocene–TMEDA.[26] *n*-Butyllithium (160 mL, 2.3 M) in *n*-hexane was added to 30 g (0.16 mol) of ferrocene dissolved in 200 mL of hexane, followed by 30 mL (0.20 mol) of TMEDA. The reaction was allowed to proceed overnight, ca. 16 h. The product was filtered off, washed with 3 × 100 mL of hexane, and dried under vacuum. This gave 44.9 g (92% yield) of an orange, pyrophoric powder.

c. (1,1′-Ferrocenediyl)dichlorosilane (II). A hexane slurry of 0.034 mol of 1,1′-dilithioferrocene–TMEDA was added slowly, over the course of several hours, to a large excess of $SiCl_4$ (100 mL, 0.87 mol). The reaction mixture was stirred for an additional 2 h, then solvent and unreacted $SiCl_4$ were removed under vacuum. This produced a red solid which was dissolved in hexane and filtered to remove LiCl, and the solvent was removed under vacuum. The solid was purified by vacuum sublimation at room temperature to remove ferrocene and subjecting the remaining solid to vacuum distillation. The fraction collected at 80 °C (0.01 mm) gave 4.3 g (50% yield) of deep red, moisture-sensitive crystals of II; mp 73–75 °C; UV max (isooctane) 470 nm (ϵ 310), 324 (180); NMR (C_6D_6) 4.02 (m, 1) and 4.29 (m, 1) ppm downfield from Me_4Si; mass spectrum *m/z* (rel intensity) 280 (3.46), 2.81 (1.26), 282 (54.61), 283 (12.02), 284 (46.12), 285 (9.52), 286 (10.98).

Anal. Calcd for $C_{10}H_8FeSiCl_2$: C, 42.43; H, 2.83; Cl, 25.07; Si, 9.93. Found: C, 42.44; H, 2.90; Cl, 25.30; Si, 10.22.

d. 1,1′-Bis(triethoxysilyl)ferrocene (III). A hexane slurry of 0.029 mol of 1,1′-dilithioferrocene–TMEDA was added slowly, over the course of several hours, to an excess of $ClSi(OCH_2CH_3)_3$ (75 mL, 0.38 mol), producing a deep red solution. The solution was stirred for several hours and filtered to remove LiCl. The solvent was removed under vacuum and the unreacted $ClSi(OCH_2CH_3)_3$ removed by vacuum distillation. The resulting red liquid was purified by short-path vacuum distillation. The fraction boiling at 70 °C (0.1 mm) was collected, yielding 5 mL (7.2 g, 50% yield) of a red liquid, III: UV max (isooctane) 440 nm (ϵ 120), 328 (90); NMR (C_6D_6) 1.02 (t, 18, $-CH_3$), 3.91 (q, 12, $-CH_2-$), 4.39 (t, 4), 4.63 (t, 4) ppm downfield from Me_4Si; mass spectrum *m/z* (rel intensity) 508 (9.08), 509 (3.93), 510 (100), 511 (37.91), 512 (17.79), 513 (5.03), 514 (1.35).

Anal. Calcd for $C_{22}H_{38}FeSi_2O_6$: C, 51.78; H, 7.45; Si, 10.98; Fe, 10.95. Found: C, 51.77; H, 7.40; Si, 10.98; Fe, 11.09.

2. Electrochemistry. Derivatized electrodes were characterized by cyclic voltammetry in CH_3CN solution of 0.1 M $(n\text{-}Bu_4N)ClO_4$ under argon at 298 K. Measurements were taken using the standard three-electrode arrangement in a one-compartment cell and all potentials were measured vs. the SCE. The counterelectrode in all cases was Pt. Cyclic voltammetry was done using a PAR Model 175 Universal Programmer, a PAR Model 173/179 potentiostat, and a Houston Instruments Model 2000 recorder.

3. Preparation of Derivatized Pt Electrodes. Two types of Pt electrodes were used, disk and foil, both of exposed area of ca. 0.3 cm^2. The disk electrodes were polished with 305 Al_2O_3 (5 μ) powder, then with 0.3-μ polishing powder until a mirror finish was obtained. The foil electrodes were simply dipped in concentrated HNO_3 for 5 min. Both types of electrodes were treated according to the published procedure[13a] to produce a surface capable of derivatization.

Electrodes derivatized with I and II were prepared by dipping the pretreated Pt electrode into an isooctane solution ca. 0.01 M of I or II under argon. Reaction was done at 25 °C for times varying from a few minutes to a few hours. After derivatization the electrode was washed several times with isooctane, then dried in an oven at 80 °C for ca. 20 min. Compound III is qualitatively less reactive than I and II and stronger conditions were required to obtain derivatized surfaces. Pretreated electrodes were placed in a 10% isooctane solution of III (~0.3 M) under argon. The reaction was carried out at 85 °C for times varying from a few hours to a few days. After derivatization, the electrode was washed several times with isooctane, then dried in an oven at 80 °C for times between 20 and 45 min. This final step seemed to be important in obtaining persistent surfaces of this compound. Those electrodes held in the oven for longer periods of time showed more persistent surface waves.

4. Preparation of Derivatized Au Electrodes. The Au working electrodes were prepared in the following way. Au foil (0.002 in. thick) was cut in rectangular pieces to ultimately expose 0.2–1.0 cm^2 of area. The Au pieces were pierced and a copper wire as a lead was attached and made secure with conducting Ag epoxy. The connection and copper wire were insulated from the solution by covering with epoxy and encasement in a 3-mm (i.d.) glass tube. The electrode was then used after cleansing in concentrated HNO_3 or was pretreated and derivatized according to the procedure in the text.

Acknowledgments. We thank the U.S. Department of Energy, Office of Basic Energy Sciences, for support of this work. M.S.W. acknowledges support as a Dreyfus Teacher–Scholar grant recipient, 1975–1980, and L.N. acknowledges the support of the CNRS, France. We wish to acknowledge useful discussions with Professors Alan Davison and Dietmar Seyferth and Dr. Alan Rudie regarding the synthesis and characterization of complexes I–III.

References and Notes

(1) M. S. Wrighton, R. G. Austin, A. B. Bocarsly, J. M. Bolts, O. Haas, K. D. Legg, L. Nadjo, and M. C. Palazzotto, *J. Electronanal. Chem.*, **87**, 429 (1978).
(2) M. S. Wrighton, R. G. Austin, A. B. Bocarsly, J. M. Bolts, O. Haas, K. D. Legg, L. Nadjo, and M. C. Palazzotto, *J. Am. Chem. Soc.*, **100**, 1602 (1978).
(3) B. F. Watkins, J. R. Behling, E. Kariv, and L. L. Miller, *J. Am. Chem. Soc.*, **97**, 3549 (1975).
(4) P. R. Moses, L. Wier, and R. W. Murray, *Anal. Chem.*, **47**, 1882 (1975).
(5) R. F. Lane and A. T. Hubbard, *J. Phys. Chem.*, **77**, 1401, 1411 (1973); **81**, 734 (1977).
(6) A. P. Brown, C. Koval, and F. C. Anson, *J. Electroanal. Chem.*, **72**, 379 (1976).
(7) (a) R. J. Burt, G. J. Leigh, and C. J. Pickett, *J. Chem. Soc., Chem. Commun.*, 940 (1976); (b) G. J. Leigh and C. J. Pickett, *J. Chem. Soc., Dalton, Trans.*, 1797 (1977).
(8) H. Landrum, R. T. Salmon, and F. M. Hawkridge, *J. Am. Chem. Soc.*, **99**, 3154 (1977).
(9) (a) L. L. Miller and M. R. Van DeMark, *J. Am. Chem. Soc.*, **100**, 639 (1978); (b) B. E. Firth, L. L. Miller, M. Mitani, T. Rogers, R. W. Murray and J. Lennox,

ibid., **98**, 8271 (1976); (c) B. E. Firth and L. L. Miller, *ibid.*, **98**, 8273 (1976); (d) M. R. Van De Mark and L. L. Miller, *ibid.*, **100**, 3223 (1978).
(10) (a) N. R. Armstrong, A. W. C. Lin, M. Fujihira, and T. Kuwana, *Anal. Chem.*, **48**, 741 (1976); (b) J. F. Evans, T. Kuwana, M. T. Henne, and G. P. Royer, *J. Electroanal. Chem.*, **80**, 409 (1977).
(11) (a) A. Diaz, *J. Am. Chem. Soc.*, **99**, 5838 (1977); (b) A. F. Diaz, U. Hetzler, and E. Kay, *ibid.*, **99**, 6780 (1977).
(12) (a) M. Fujihira, T. Matsue, and T. Osa, *Chem. Lett.*, 875 (1976); (b) T. Osa and M. Fujihira, *Nature (London)*, **264**, 349 (1976); (c) M. Fujihira, A. Tamura, and T. Osa, *Chem. Lett.*, 361 (1977); (d) M. Fujihira, N. Ohishi, and T. Osa, *Nature (London)*, **268**, 226 (1977).
(13) (a) J. R. Lenhard and R. W. Murray, *J. Electroanal. Chem.*, **78**, 195 (1977); (b) P. R. Moses and R. W. Murray, *J. Am. Chem. Soc.*, **98**, 7435 (1976); *J. Electroanal. Chem.*, **77**, 393 (1977); (c) C. M. Elliott and R. W. Murray, *Anal. Chem.*, **48**, 1247 (1976); (d) D. G. David and R. W. Murray, *Ibid.*, **49**, 194 (1977); (e) J. C. Lennox and R. W. Murray, *J. Electroanal. Chem.*, **78**, 395 (1977).
(14) (a) A. P. Brown and F. C. Anson, *Anal. Chem.*, **49**, 1589 (1977); *J. Electroanal. Chem.*, **83**, 203 (1977); (b) C. A. Koval and F. C. Anson, *Anal. Chem.*, **50**, 223 (1978).
(15) (a) K. S. V. Santhanam, J. Jespersen, and A. J. Bard, *J. Am. Chem. Soc.*, **99**, 274 (1977); (b) A. Merz and A. J. Bard, *ibid.*, **100**, 3222 (1978), and private communication.
(16) J. M. Bolts and M. S. Wrighton, *J. Am. Chem. Soc.*, **100**, 5257 (1978).
(17) J. M. Bolts, A. B. Bocarsly, M. C. Palazzotto, E. G. Walton, N. S. Lewis, and M. S. Wrighton, submitted for publication.
(18) Y. S. Sohn, D. N. Hendrickson, and H. B. Gray, *J. Am. Chem. Soc.*, **93**, 3603 (1971).
(19) (a) A. G. Osbourne and R. H. Whitely, *J. Organomet. Chem.*, **101**, C27 (1975); (b) H. Stoeckli-Evans, A. G. Osbourne, and R. H. Whitely, *Helv. Chim. Acta*, **59**, 2402 (1976).
(20) G. J. Janz and R. P. T. Tomkins, "Nonaqueous Electrolytes Handbook", Vol. II, Academic Press, New York, N.Y., 1973, and references cited therein.
(21) E. Laviron, *J. Electroanal. Chem.*, **39**, 1 (1972).
(22) R. S. Nicholson and I. Shain, *Anal. Chem.*, **36**, 706 (1976), and references cited therein.
(23) W. H. Morrison, Jr., S. Krogsrud, and D. N. Hendrickson, *Inorg. Chem.*, **12**, 1998 (1973).
(24) T. Dickinson, A. F. Povey, and P. M. A. Sherwood, *J. Chem. Soc., Faraday Trans. 1*, **71**, 299 (1975).
(25) D. Seyferth, H. P. Hoffman, R. Burton, and J. F. Helling, *Inorg. Chem.*, **1**, 227 (1962).
(26) J. C. Smart, Ph.D. Thesis, Massachusetts Institute of Technology, 1974.

Crystallographic Determination of the Absolute Configuration at Iron of a Series of Chiral Iron Alkyls. Empirical Circular Dichroism Spectroscopic Correlations

Chaw-Kuo Chou, David L. Miles, Robert Bau,*[1a] and Thomas C. Flood*[1b]

Contribution from the Department of Chemistry, University of Southern California, University Park, Los Angeles, California 90007. *Received November 9, 1977*

Abstract: The absolute configurations of two optically active iron complexes, $(+)_{578}$-CpFe(CO)(PPh_3)(CH_2O-menthyl) (**1**) and $(+)_{578}$-CpFe(CO)(PPh_3)(CH_2COO-menthyl) (**2**), have been determined by single-crystal X-ray diffraction methods and have been correlated with their circular dichroism spectra. The configuration of **1** is *S* and that of **2** is *R* (based on the sequencing rules proposed recently by Stanley and Baird). Anomalous dispersion effects were used to elucidate the absolute configuration of **1**, while that of **2** was determined using the (−)-menthyl group as a reference. From these results, the absolute configurations of a large number of complexes of the type CpFe(CO)(PPh_3)(X) can be deduced and compared to their CD spectra [X = Br, I, Me, Et, *n*-Pr, *i*-Bu, CH_2-c-C_3H_5, CH_2Cl, CH_2Br, CH_2I, CH_2Ph, C(O)Me, $S(O)_2R$, $CH_2S(O)_2O$(menthyl), (η^2-C_2H_4)$^+BF_4^-$]. It is concluded that the maxima found at the 300–350- and 350–450-nm regions of the CD spectra can serve as a reliable indicator of the absolute configuration at iron, provided that the X groups are not too dissimilar. Crystal details: **1**-*S* crystallizes in space group $P2_1$ (monoclinic) with a = 10.882 (3) Å, b = 11.054 (4) Å, c = 13.664 (4) Å, β = 102.66 (2)°, V = 1603.7 Å^3, Z = 2; **2**-*R* crystallizes in space group $P\bar{1}$ (triclinic) with a = 7.660 (1) Å, b = 13.806 (1) Å, c = 15.948 (1) Å, α = 108.23 (1)°, β = 88.62 (1)°, γ = 95.06 (1)°, V = 1595.5 Å^3, Z = 2. Final agreement factors are for **1**-*S*, R = 6.2% (3655 reflections); for **2**-*R*, R = 8.4% (3665 reflections).

Introduction

Detailed understanding of the chemistry of any element which may exist in a chiral bonding environment requires development of methods of synthesis and resolution of this chiral center, and thorough investigation of the stereochemical consequences of its various characteristic reaction types. It is necessary to establish the absolute configuration of a number of molecules, to accumulate a basic set of reactions of known stereochemical outcome, and to correlate chiroptical properties with absolute configuration.

A sizable body of data is now available for molecules containing chiral silicon, phosphorus, and sulfur, and for chiral coordination complexes of the transition elements. In the rapidly maturing area of organotransition metal chemistry, however, only relatively recently has attention turned toward investigations based on resolution of chiral metal centers.[2-8]

Because $CpFe(CO)_2X$ systems (Cp ≡ η^5-C_5H_5; X is a wide variety of functional groups) are synthetically so accessible and are so well behaved experimentally, they have been the object of considerable synthetic and mechanistic investigation. The metal alkyls $CpFe(CO)_2R$ have been valuable as model compounds in the examination of the chemistry of the metal–carbon σ bond.[9] In the same way, $CpFe(CO)(PR_3)X$ compounds have significant potential for use in this area because of their chirality. Such molecules are generally nonlabile to dissociation under ambient conditions, and therefore tend to be optically stable. A number of these chiral iron molecules have already been resolved, and have yielded useful mechanistic information.[3-6]

Because of the potential interest of these chiral iron systems, we have established the absolute configuration of two iron alkyls, (*S*)-**1** and (*R*)-**2**, by X-ray crystallographic structure determinations.[10] This paper describes these structures, and also describes the circular dichroism spectra of these and a number of other derivatives $CpFe(CO)(PPh_3)X$ which we have prepared. In this way, the absolute configuration at iron of at least 12 such compounds has been established. In addition to our work, the absolute configurations of (*S*)-[CpFe(CO)(PPh_3){C((*S*)=N^+HCHMePh)Me}]BF_4^- (**3**)[11] and (*S*)-

0002-7863/78/1500-7271$01.00/0